Novel partial common bile duct ligation procedure in rats with reduced mortality and delayed onset of cirrhosis

WANRONG XIA[1,2*], HONGJI YAO[1*], TONGXIN MU[1], HUI LIU[1,2], JIANHUA CHEN[3], SHI FENG[4] and SHILEI WEN[1,2]

[1]Key Laboratory of Tropical Translational Medicine of Ministry of Education and Key Laboratory of Brain Science Research Transformation in Tropical Environment of Hainan Province, School of Basic Medicine and Life Sciences, Hainan Medical University, Haikou, Hainan 571199, P.R. China; [2]Department of Human Anatomy, College of Basic Medicine and Life Sciences, Hainan Medical University, Haikou, Hainan 571199, P.R. China; [3]Department of Forensic Medicine, College of Basic Medicine and Life Sciences, Hainan Medical University, Haikou, Hainan 571199, P.R. China; [4]Department of Histology and Embryology, Basic Medical School, Kunming University of Science and Technology, Kunming, Yunnan 650500, P.R. China

Received January 22, 2025; Accepted June 11, 2025

DOI: 10.3892/etm.2025.12917

Abstract. Common bile duct ligation (BDL) in rats is a widely used animal model for the study of cholestatic liver injury; however, it has a high mortality rate and leads to rapid disease progression. To address these limitations, the present study developed a simplified partial BDL (p-BDL) procedure by inserting a 26G disposable venous indwelling needle during ligation of the common bile duct, and subsequently removing the needle to create a narrow passage through the ligature points. The rats were euthanized 1 or 2 months after the procedure for histological, immunohistochemical and gelatin zymography analyses of the liver. Notably, no animals died during the experimental period, demonstrating the low mortality rate of the model. When assessed 1 month post-p-BDL, the rats exhibited mild liver fibrosis, while at 2 months, severe liver fibrosis was observed. Corresponding changes in liver function indices were also noted. Specifically, markers of liver fibrosis, including collagen I, collagen III and α-smooth muscle actin, as well as matrix metalloproteinase (MMP)-2 and MMP-9, which contribute to extracellular matrix degradation, were significantly upregulated following p-BDL. These findings are similar to those observed following BDL, and indicate that the p-BDL model was successfully established. This model mitigates the drawbacks of traditional BDL and mimics chronic cholestatic cirrhosis, as observed clinically.

Correspondence to: Dr Shilei Wen, Key Laboratory of Tropical Translational Medicine of Ministry of Education and Key Laboratory of Brain Science Research Transformation in Tropical Environment of Hainan Province, School of Basic Medicine and Life Sciences, Hainan Medical University, 3 Xueyuan Road, Longhua, Haikou, Hainan 571199, P.R. China
E-mail: wenshl2005@126.com

Dr Shi Feng, Department of Histology and Embryology, Basic Medical School, Kunming University of Science and Technology, 727 Jingming South Road, Chenggong, Kunming, Yunnan 650500, P.R. China
E-mail: jetmork@126.com

*Contributed equally

Abbreviations: p-BDL, partial bile duct ligation; MPO, month post operation; AST, aspartate aminotransferase; ALT, alanine aminotransferase; TBIL, total bilirubin; H&E, hematoxylin and eosin; CK-19, cytokeratin 19; α-SMA, a-smooth muscle actin; MMP, matrix metalloproteinase

Key words: bile duct ligation, cholestatic cirrhosis, partial bile duct ligation

Introduction

The common bile duct ligation (BDL) model in rats is one of most widely used animal models for the study of cholestatic liver injury (1,2). The BDL procedure involves the excision or ligation of the common bile duct, resulting in obstruction of bile flow. This leads to intrahepatic bile duct hyperplasia, accompanied by inflammatory infiltration and fibrous deposition (3). BDL possesses several advantages, including technical simplicity, ease of replication, low cost and the rapid development of liver damage (4,5). Nevertheless, due to rapid development, the liver lesions of BDL more closely resemble acute bile duct obstruction, which is rare in clinical cases (6,7). Also, they differ from those of chronic cholestatic liver diseases, particularly those in which cholangiocytes are the primary targets of injury, as observed in cholangiopathies (8). In addition, complications such as bile leakage, intestinal adhesions, biliary cyst rupture and bile acid toxicity may occur, resulting in a mortality rate of >20% beyond 5-6 weeks post-surgery (9-11). Furthermore, in some cases, mortality rates can reach more than 30% within 2 weeks (3). Therefore, modifications of the BDL procedure are necessary to reduce mortality and delay the onset of cirrhosis, to more accurately simulate cholestatic cirrhosis in patients.

A 26G (0.60x15 mm) disposable venous indwelling needle or cannula consists of a flexible plastic trocar and a rigid metal needle core. In the present study, it was hypothesized that if the trocar is placed above the common bile duct prior to ligation and the needle core is subsequently withdrawn, this will leave a channel within the ligated common bile duct. This may allow the channel to gradually expand due to the rapid increase in bile duct pressure after ligation, enabling bile to be slowly discharged and reducing bile duct pressure. This modification may have the potential to reduce animal mortality and delay the progression of cirrhosis.

Based on this approach, a partial BDL (p-BDL) model was established in rats by embedding a trocar and then ligating the common bile duct. The study investigated the ability of this model to slow the progression of liver fibrosis and decrease mortality in animal subjects compared with that of the traditional BDL model.

Materials and methods

Animals and groups. The study was approved by The Ethics Committee of Hainan Medical University (Haikou, China; approval no. HYLL-2021-346). A total of 30 male Wistar rats (age, 6-8 weeks; weight, 200-220 g) were obtained from The Experimental Animal Center of Guangdong Province (Guangzhou, China). Animals were fed in a barrier environment, under a 12-h light-dark cycle, at a constant temperature of 24±2˚C and relative humidity ranging from 50-65%, with free access to chow and water. The animals were acclimatized to the laboratory conditions for 1 week prior to surgery.

The rats were randomly divided into the following three groups (n=10/group): i) Sham group; ii) 1 month post operation (MPO) group; and iii) 2 MPO group. Animals in the 1 MPO and 2 MPO groups underwent p-BDL, whilst animals in the sham group underwent laparotomy but without p-BDL.

Modeling procedure. The rats fasted for ~12 h prior to surgery. Anesthesia was induced with 2% pentobarbital sodium (40 mg/kg intraperitoneally), and the animals were bound in a supine position on the operating board following the confirmation of complete anesthesia (Fig. 1A). Next, the abdominal hair was moistened with soapy water and removed using a razor, taking care to prevent skin injury. The scope of skin preparation extended from the xiphoid process to the iliac crest, and laterally to the midclavicular lines. Subsequently, the surgical area was disinfected with iodophor (Fig. 1B). An incision was made along the abdominal white line ~1 cm below the xiphoid process, and the abdominal wall muscles were incised along the same line using tissue scissors to open the abdominal cavity. The incision was ~5 cm in length (Fig. 1C). Two sterile cotton swabs were then moistened with saline and used to move the intestines towards the right lower abdomen. The duodenum and common bile duct were identified and gently pulled downward to straighten the common bile duct. A saline-soaked gauze pad was placed beneath the incision to maintain intestinal moisture (Fig. 1D). Next, three ligatures were placed loosely around the common bile duct using 3-0 black silk sutures, with an interval of ~2 mm between adjacent ligatures (Fig. 1E).

The modeling procedure was carried out using a 26G (0.60x15 mm) disposable venous indwelling needle (cat. no. Y-shaped IV-Y26II; Jiangxi Fenglin Medical Technology Co., Ltd.). Prior to insertion, the metal core was withdrawn by ~2 mm, ensuring that the tip of the needle was concealed within the casing to avoid injury to surrounding tissues. The trocar was then positioned above the common bile duct, and the three previously placed surgical sutures were knotted closely around it. The tensile force of the surgical knots was measured to be ~5 kg using a tension meter (Fig. 1F). Following ligation, the metal core was gently extracted, and the excess portion of the cannula was cut off. Approximately 3 mm of the tip and end of the casing was left exposed beyond the ligature points on both sides (Fig. 1G). Finally, a cotton swab was used to move the intestines back into the abdominal cavity and restore them to their original position (Fig. 1H), and the muscle and skin were then sutured sequentially (Fig. 1I). After the surgery, the rats were placed in a cage, kept warm and allowed to wake up. A regular diet was provided, and each rat received a daily intraperitoneal injection of 200,000 units penicillin sodium for three consecutive days to prevent infection.

Euthanasia and sampling. Animals in the sham and 1 MPO groups were euthanized 1 month post-surgery, while those in the 2 MPO group were euthanized 2 months post-surgery. The 1-2-month postoperative period was selected based on a previous review which indicates that this is a critical time for the progression of hepatic fibrosis and metabolic decompensation (2). Following surgery, the model rats exhibited a noticeable yellow discoloration of the fur, particularly at 2 months post-surgery (Fig. 2A), which was indicative of severe jaundice. Therefore, 1 and 2 months post-surgery were designated as the humane endpoints of the study. All animals were euthanized by cardiac exsanguination following anesthesia with pentobarbital sodium (150 mg/kg intraperitoneally). Death was confirmed by the absence of pain responses, complete cessation of cardiac and respiratory activity, and pupil dilation. Liver tissues were obtained and either fixed with 4% paraformaldehyde at 4˚C for 48 h and embedded in paraffin for histological experiments or snap-frozen in liquid nitrogen and stored at -80˚C for zymography. Serum samples were centrifuged at 2,000 x g for 10 min at 4˚C and then stored at -20˚C.

Histological detection. Paraffin-embedded liver sections (3 μm) were subjected to staining with hematoxylin and eosin (H&E), Sirius red (cat. no. PH1098; Fuzhou Phygene Biotechnology, Co., Ltd.) and Masson's trichrome stain (cat. no. DC0032; Leagene; Beijing Regen Biotechnology Co., Ltd.). The staining procedure was performed as previously described (12). Stained sections were viewed under a microscope (Olympus BX53; Olympus Corporation). For each section, five fields of view were randomly selected and analyzed using Image-Pro Plus 6.0 software (Media Cybernetics, Inc.). The degree of hepatic fibrosis was assessed using Ishak's scoring system (13), which ranges from 0-6, with higher scores denoting more severe fibrosis.

Immunohistochemical analysis. Cytokeratin 19 (CK-19) protein is a recognized marker of biliary epithelial cells and

Figure 1. Representative images of the partial common bile duct ligation procedure. (A) Rat bound in a supine position; (B) skin preparation and disinfection; (C) opening of the abdominal cavity; (D) exposure of the bile duct; (E) insertion of the surgical sutures; (F) binding the trocar; (G) pulling out the needle core and cutting off the cannula; (H) pushing the intestine back into the abdomen; (I) closing the abdomen layer by layer.

is associated with the progression of liver fibrosis (3). In the present study, immunohistochemical staining of CK-19 was performed to investigate intrahepatic biliary cell proliferation. Liver fibrosis was further evaluated by the immunohistochemical staining of collagen I, collagen III and α-smooth muscle actin (α-SMA). In addition, the expression levels of matrix metalloproteinase (MMP)-2 and -9 are significantly upregulated in liver fibrosis and commonly used as biomarkers to assessing the extent of fibrotic progression (14). Therefore, the expression levels of MMP-2 and -9 were also evaluated by immunohistochemistry (IHC).

After dewaxing and hydration using xylene and a descending alcohol series, 3 μm thick liver sections were incubated with 3% H_2O_2 at room temperature for 10 min to quench endogenous peroxidase activity. The sections were then blocked with 10% goat serum (cat. no. PV-9001; Beijing Zhongshan Jinqiao Biotechnology Co., Ltd.) at room temperature for 15 min. Subsequently, the sections were incubated overnight at 4˚C with the following diluted primary antibodies: CK-19 (1:800; cat. no. 10712-1-AP), collagen I (1:800; cat. no. 14695-1-AP), collagen III (1:3,200; cat. no. 22734-1-AP), α-SMA (1:1,600; cat. no. 14395-1-AP), MMP-2 (1:400; cat. no. 10373-2-AP) and MMP-9 (1:800; cat. no. 10375-2-AP), all from Proteintech Group, Inc. The samples were subsequently incubated with a horseradish peroxidase-conjugated secondary antibody (ready-to-use; cat. no. PV-9001) at 37˚C for 30 min. Finally, antigen detection was performed using a Diaminobenzidine Substrate Kit (cat. no. ZLI-9018; Beijing Zhongshan Jinqiao Biotechnology Co., Ltd.). Positive staining was visualized as brown staining on the cytomembrane. Under a light microscope (Olympus BX53; Olympus Corporation), five fields of view were randomly selected from each section for analysis, and analyzed using the software of Image-Pro Plus 6.0 (Media Cybernetics, Inc.).

Assessment of MMP activities by gelatin zymography. The gelatinolytic activities of intrahepatic MMPs were investigated using gelatin zymography as previously described (15). This assay detects the proenzyme, active enzyme, active fragments and complex forms of gelatinases based on their distinct molecular weights. Equal amounts of non-denatured protein (20 μg) from each liver sample were mixed with 2X SDS loading buffer (without reducing agent) and subjected to SDS-PAGE on 8% gels containing 1 mg/ml gelatin (MilliporeSigma). After electrophoresis, the gels were washed four times (15 min/wash) in 2.5% Triton X-100 at room temperature to remove SDS. The gels were then incubated at 37˚C in incubation buffer containing 50 mM Tris-HCl, 5 mM $CaCl_2$, 1 μM $ZnCl_2$ and 0.02% Brij-35 at pH 7.5 for ~24 h. Subsequently, the gels were stained with Coomassie Brilliant Blue R250 (0.25%) in 30% methanol and 10% acetic acid for ~1 h at room temperature, then destained overnight with 30% methanol and 10% acetic acid at room temperature to clearly visualize the digested bands. Proteolytic activities of MMPs were visualized as clear bands against the blue background of stained gelatin. Proteolytic activities were normalized to those of total proteins, as assessed by Coomassie Brilliant Blue R250 staining of the SDS-PAGE gels, and were analyzed using Quantity One (Version 4.6.2; Bio-Rad Laboratories, Inc.).

Serum test. To assess the impact of p-BDL on liver function, the following parameters were analyzed using the specified kits: Total bilirubin (TBIL; cat. no. G1224W), aspartate aminotransferase (AST; cat. no. G0424W) and alanine aminotransferase (ALT; cat. no. G0423W). All kits were from Suzhou Grace Biotechnology Co., Ltd. The results were obtained using a microplate reader (Epoch 2; Agilent Technologies, Inc.).

Statistical analysis. All data are presented as the mean ± standard deviation and were analyzed using SPSS 21.0 software (IBM Corporation). One-way ANOVA followed by Tukey's post hoc tests were used to analyze normally distributed continuous data and Kruskal-Wallis followed by Dunn's post hoc tests were used to analyze ordinal data. $P<0.05$ was considered to indicate a statistically significant difference.

Results

Survival rate and gross appearances in rats. One rat was excluded from the study following mortality caused by accidental hepatic portal vein puncture during the surgical procedure. No post-operative mortality occurred prior to scheduled sacrifice, indicating that the surgical safety of the p-BDL technique was markedly improved compared with that of conventional BDL.

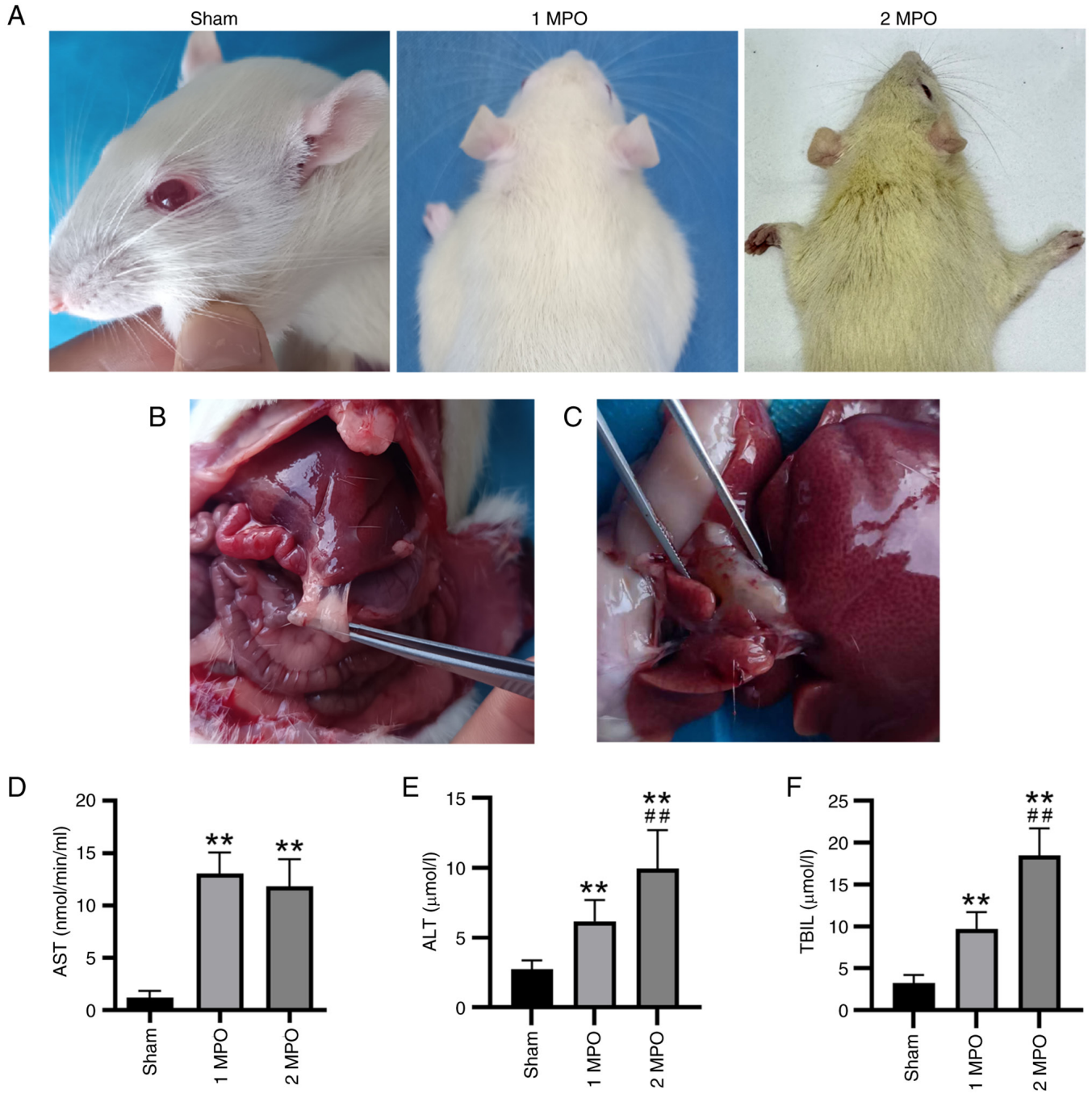

Figure 2. Gross appearance and liver function indices of the rats following partial common bile duct ligation. (A) Photographs of a representative rat from each group. (B) Adhesion between the inferior margin of the liver and the bowel. (C) Enlargement of the common bile duct. Serum levels of (D) ALT, (E) AST and (F) TBIL. All values are presented as the mean ± standard deviation (n=10). **P<0.01 vs. sham group; $^{\#\#}$P<0.01 vs. 1 MPO group. ALT, alanine aminotransferase; AST, aspartate aminotransferase; TBIL, total bilirubin; MPO, month post operation.

Prior to sacrifice, the hair color of the animals became yellowish, indicating that biliary obstruction was effectively established by the p-BDL procedure (Fig. 2A), particularly in the 2 MPO group. When the abdominal cavity was opened for sampling, adhesion between the inferior margin of the liver and the bowel was clearly observed in the surgical groups (Fig. 2B), which was indicative of an immune reaction caused by the non-absorbable surgical sutures and the plastic casing. Additionally, enlargement of the common bile duct was observed in the surgical groups, indicating the successful establishment of biliary obstruction (Fig. 2C).

p-BDL upregulated liver function markers. Serum test results revealed that the liver function indices AST, ALT and TBIL were significantly elevated in the two surgical groups (Fig. 2D-F), particularly in the 2 MPO group, compared with those in the sham group. This upregulation signified the impairment of the liver following the p-BDL procedure.

Histopathological changes of livers. H&E, Sirius red and Masson's trichrome staining of the livers were conducted to visualize the histopathological alterations and quantify the degree of liver fibrosis induced by the p-BDL procedure (Fig. 3).

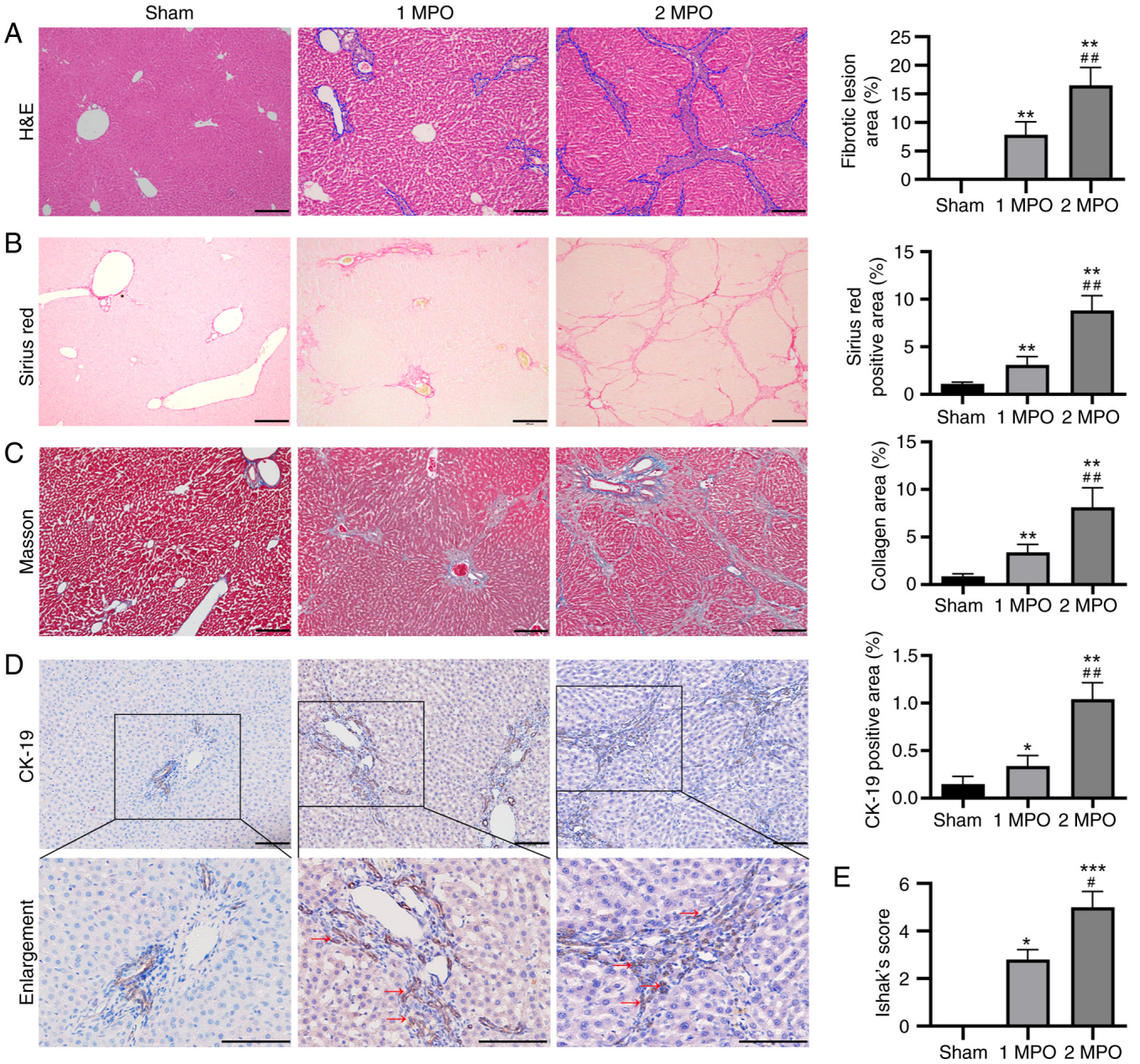

Figure 3. Histopathological changes of rat livers following partial common bile duct ligation. Representative images and histopathological analysis by (A) H&E staining, (B) Sirius red staining and (C) Masson's trichrome staining (scale bar, 200 μm; magnification, x100). (D) CK-19 immunostaining (scale bar, 100 μm; magnification, x100). (E) Ishak's scores of hepatic fibrosis based on the staining results. Blue dashed lines demarcate fibrotic tissue boundary. Red arrows demarcate pseudo bile ducts in Fig. 3D. All values are presented as the mean ± standard deviation (n=10). *P<0.05, **P<0.01 or ***P<0.001 vs. the sham group; $^{\#}$P<0.05 or $^{\#\#}$P<0.01 vs. the 1 MPO group. H&E, hematoxylin and eosin; CK-19, cytokeratin 19; MPO, month post operation.

The livers in the sham group exhibited a normal histological structure, with only a minor amount of collagen visible in the portal area (Fig. 3A). The portal areas of the livers in the 1 MPO and 2 MPO groups appeared expanded compared with those in the sham group due to pseudo bile duct proliferation, particularly in the 2 MPO group. In addition, no evidence of hepatic necrosis was observed in the 1 MPO and 2 MPO groups. Both Sirius red and Masson's trichrome staining revealed an abundant deposition of collagen in the 1 MPO and 2 MPO groups, particularly in the 2 MPO group (Fig. 3B and C). Notably, the areas of fibrotic lesions and percentages of collagen in the 1 MPO group and particularly in the 2 MPO group, were significantly higher than those in the sham group.

The biliary epithelial cells marker CK-19 was mainly expressed in normal bile duct endothelial cells in the sham group (Fig. 3D). By contrast, high expression of CK-19 was observed not only in normal bile duct cells but also in pseudo bile ducts in the 1 MPO and 2 MPO groups, indicating an abundance of reactive bile ductules in the portal regions.

Based on these staining results, Ishak's score was utilized to assess the level of liver fibrosis. The scores ranged from 0 for a normal liver to 6 for a cirrhotic liver. The sham group exhibited no fibrosis and received a score of 0. The 1 MPO group presented fibrous expansion in most of the portal area, along with occasional portal-to-portal bridging, and had an average

score of 2.8±0.42. Finally, the 2 MPO group displayed nodule formation and probable cirrhosis, and had an average score of 5.00±0.67. These results indicate that obstructive jaundice was effectively induced by p-BDL in a manner similar to that induced by BDL.

Upregulation of fibrotic markers in livers after p-BDL. IHC assays for collagen I, collagen III and α-SMA were conducted to further assess the extent of liver fibrosis. The results demonstrated that collagen I and α-SMA were only weakly expressed in the portal area in the sham group but exhibited significant increases in the 1 MPO and 2 MPO groups, with the 2 MPO group showing markedly and significantly higher expression than the 1 MPO group (Fig. 4A-C). In addition, collagen III was uniformly distributed throughout the hepatic lobules in the sham group, whereas it was abundantly expressed and significantly upregulated in the portal area and interlobular septum in the 1 MPO and 2 MPO groups.

Upregulation of MMPs in livers after p-BDL. The expression levels of MMPs were evaluated to investigate the molecular mechanisms underlying liver fibrosis following p-BDL. The IHC results demonstrated that MMP-2 and MMP-9 exhibited only minimal positivity in the sham group, whereas the number of positive cells was markedly elevated in the 1 MPO and 2 MPO groups (Fig. 4D and E). Furthermore, gelatin zymography revealed significantly increased activity of the MMP complex and MMP-9 in the liver tissues of both the 1 MPO and 2 MPO groups compared to the sham group. Additionally, active-MMP-2 activity was significantly elevated in the 2 MPO group vs. the sham group. These findings indicate severe damage to the hepatic extracellular matrix following p-BDL.

Discussion

In the present study, a model of p-BDL was established, which offers several advantages over previous BDL models. The p-BDL procedure is straightforward to conduct, highly reproducible, and associated with a low mortality rate and slow progression of liver fibrosis. These features overcome the limitations of the classic BDL model, which is characterized by high mortality rates and the rapid progression of liver damage.

In addition to complications such as bile leakage, the high mortality following conventional BDL is likely associated with acute liver failure resulting from complete bile duct obstruction. Consequently, prior studies have utilized BDL surgery to establish a liver failure model in rats (16-19). Upon the re-evaluation of the H&E staining of rat livers from our previous study (15), it was observed that BDL induced severe hepatocyte death and pathological changes, particularly in the first 2 weeks after BDL surgery. By contrast, p-BDL resulted in markedly less severe hepatocyte damage without evidence of acute liver failure.

Previous studies have shown that rats undergoing BDL surgery develop moderate liver fibrosis by 4 weeks and cirrhosis by 4-6 weeks after the surgery (1). Upon reviewing the Sirius red staining results and Ishak's scores from our previous BDL study, as well as those reported by other researchers, it was observed that the p-BDL model led to lower degrees of liver fibrosis and bile duct hyperplasia 1 month after surgery compared with those observed just 2 weeks after BDL surgery (15,20,21). In addition, the degrees of hepatic fibrosis and bile duct hyperplasia 2 months after the p-BDL surgery were similar to those 3-6 weeks following BDL surgery (3,15,22-24).

Collagen I, collagen III and α-SMA, which are commonly utilized markers of liver fibrosis, were found to be significantly upregulated following p-BDL surgery in the present study. This finding is consistent with the results observed after conventional BDL surgery (20), suggesting that p-BDL and BDL induce comparable extracellular matrix alterations. Previous research has demonstrated that the elevation of MMPs during liver fibrosis typically reflects degradation of the normal hepatic extracellular matrix (25). This is supported by the upregulated activity of MMPs in the present study, which aligns with the findings from our previous study on BDL (15). In summary, the rat p-BDL model established in the present study exhibits similarities to the conventional BDL model in terms of fibrotic deposition characteristics and underlying molecular changes.

While this p-BDL procedure yielded significant outcomes, certain limitations require consideration. Firstly, during the experimental period, no mortality was observed in rats within 2 months post p-BDL surgery. However, one intraoperative death occurred due to accidental puncture of the portal vein during the placement of sutures beneath the common bile duct, resulting in fatal hemorrhage. The portal vein and common bile duct are anatomically proximate structures separated by only 2-3 mm in rats (26). Therefore, meticulous surgical technique is required to prevent iatrogenic injury to adjacent vasculature or organs, which could lead to procedural complications or animal mortality (27). Secondly, although the operator underwent rigorous clinical training and utilized triple ligations to reduce ligation-point relaxation during BDL, certain risks of surgical failure remain. Specifically, bile duct recanalization may occur as a result of suture slippage or loosening at the ligation sites, which could compromise the integrity of the surgery. To mitigate this, the adjunctive application of biological glue at the ligation points is proposed to stabilize the sutures and maintain consistent tension, thereby enhancing surgical success rates. Future experiments will rigorously validate this hypothesis through the systematic quantification of post-operative outcomes, including but not limited to the measurement of bile outflow rates. In addition, the present study only used Wistar rats, and it remains unclear whether the results are applicable to other rat strains. The anatomy of the liver and biliary tract is reported to be similar across different rat strains (26). Therefore, in subsequent studies on the treatment of liver fibrosis in rats, the p-BDL surgery will be applied to other rat strains, such as Sprague-Dawley rats, to evaluate the universality and applicability of this surgical method.

Although numerous modifications have been proposed to enhance BDL, their widespread adoption has been hindered by various challenges. For example, reversible BDL surgery requires a second procedure, is technically complex, exhibits a high mortality rate and has the potential to induce biliary tract infection or abdominal infection (28-31). In another study, a medical adhesive gel was injected into the bile duct to create a bile duct obstruction model (32). Although this enhanced

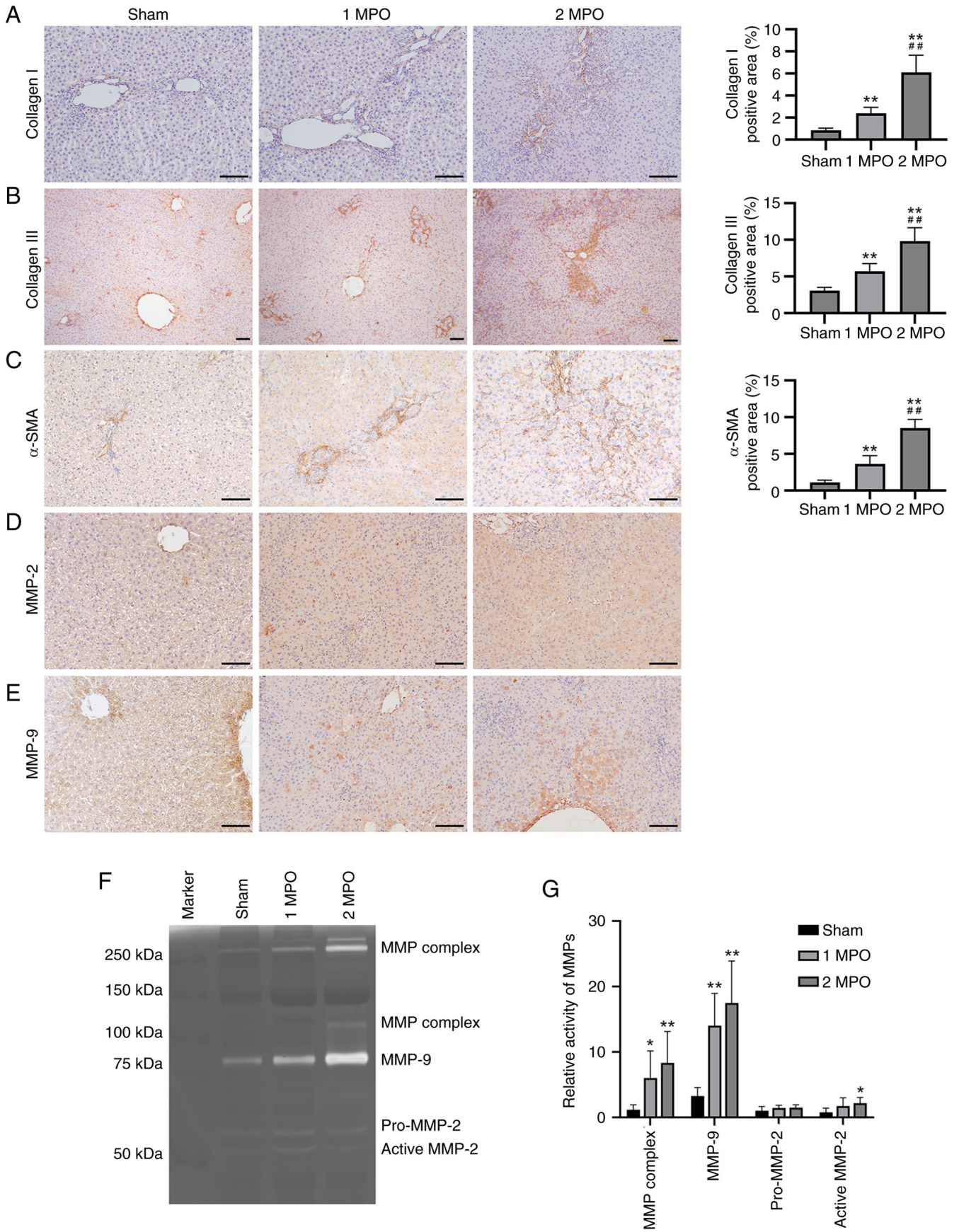

Figure 4. Upregulation of fibrotic markers and MMPs in rat livers following partial common bile duct ligation. Representative IHC staining images and quantification of (A) collagen I, (B) collagen III and (C) α-SMA. Representative IHC staining images of (D) MMP-2 and (E) MMP-9. (A-E) Scale bar, 100 μm; magnification, x100. (F) Representative gelatin zymography results and (G) the relative activities of MMP complex, pro-MMP-2, active MMP-2 and MMP-9 in the rat livers. All values are presented as mean ± standard deviation (n=5). *P<0.05 or **P<0.01 vs. the sham group; $^{\#\#}$P<0.01 vs. the 1 MPO group. MMP, matrix metalloproteinase; IHC, immunochemistry; SMA, smooth muscle actin; MPO, month post operation.

the survival rate, the progression of the disease appeared to be accelerated. Furthermore, Apostu *et al* (33) attempted to create a model of selective obstructive cholestasis in rats by ligating two of the four liver lobes, to create two cholestatic liver lobes and leave two healthy lobes as a control. However, insufficient evidence was obtained to demonstrate that the surgery achieved its intended goal.

In conclusion, the present study successfully established a p-BDL procedure, which can overcome certain flaws of the traditional BDL surgery. However, further research is necessary to confirm the reliability and feasibility of this technique.

Acknowledgements

Not applicable.

Funding

The present study was supported by a grant from Natural Science Foundation of Hainan Province (grant no. 821RC570).

Availability of data and materials

The data generated in the present study may be requested from the corresponding author.

Authors' contributions

WX established the animal models, analyzed the data and wrote the original manuscript. HY and HL performed experiments and analyzed the experimental data. TM and JC analyzed the experimental data, and JC also guided the experiments. SF designed the study, guided the experiments and revised the manuscript. SW contributed to funding acquisition and project administration, designed the study, and revised the manuscript. All authors read and approved the final version of the manuscript. WX and SW confirm the authenticity of all the raw data.

Ethics approval and consent to participate

This study was approved by The Ethics Committee of Hainan Medical University (approval no. HYLL-2021-346).

Patient consent for publication

Not applicable.

Competing interests

The authors declare that they have no competing interests.

Authors' information

Shilei Wen, ORCID: 0000-0001-9329-6709; Shi Feng, ORCID: 0000-0003-4015-2204.

Use of artificial intelligence tools

During the preparation of this work, artificial intelligence tools were used to improve the readability and language of the manuscript, and subsequently, the authors revised and edited the content produced by the artificial intelligence tools as necessary, taking full responsibility for the ultimate content of the present manuscript.

References

1. Wu S, Wang X, Xing W, Li F, Liang M, Li K, He Y and Wang J: An update on animal models of liver fibrosis. Front Med (Lausanne) 10: 1160053, 2023.
2. Faccioli LAP, Dias ML, Paranhos BA and Dos Santos Goldenberg RC: Liver cirrhosis: An overview of experimental models in rodents. Life Sci 301: 120615, 2022.
3. Zeng Z, Lei Y, Yang C, Wu X, Zhang L, Yang Z, Chen L, Wang X, Belguise K, Li Y and Yi B: The therapeutic effects of baicalein on the hepatopulmonary syndrome in the rat model of chronic common bile duct ligation. J Clin Transl Hepatol 12: 496-504, 2024.
4. Perlman RL: Mouse models of human disease: An evolutionary perspective. Evol Med Public Health 2016: 170-176, 2016.
5. Lee YS and Seki E: In vivo and in vitro models to study liver fibrosis: Mechanisms and limitations. Cell Mol Gastroenterol Hepatol 16: 355-367, 2023.
6. Mariotti V, Cadamuro M, Spirli C, Fiorotto R, Strazzabosco M and Fabris L: Animal models of cholestasis: An update on inflammatory cholangiopathies. Biochim Biophys Acta Mol Basis Dis 1865: 954-964, 2019.
7. Kolaric TO, Kuna L, Covic M, Roguljic H, Matic A, Sikora R, Hefer M, Petrovic A, Mihaljevic V, Smolic R, *et al*: Preclinical models and promising pharmacotherapeutic strategies in liver fibrosis: An update. Curr Issues Mol Biol 45: 4246-4260, 2023.
8. Marques TG, Chaib E, da Fonseca JH, Lourenço AC, Silva FD, Ribeiro MA Jr, Galvão FH and D'Albuquerque LA: Review of experimental models for inducing hepatic cirrhosis by bile duct ligation and carbon tetrachloride injection. Acta Cir Bras 27: 589-594, 2012.
9. Smith GP: Animal models of cutaneous and hepatic fibrosis. Prog Mol Biol Transl Sci 105: 371-409, 2012.
10. Starkel P and Leclercq IA: Animal models for the study of hepatic fibrosis. Best Pract Res Clin Gastroenterol 25: 319-333, 2011.
11. Bao YL, Wang L, Pan HT, Zhang TR, Chen YH, Xu SJ, Mao XL and Li SW: Animal and organoid models of liver fibrosis. Front Physiol 12: 666138, 2021.
12. Feng S, Tong H, Gao JH, Tang SH, Yang WJ, Wang GM, Zhou HY and Wen SL: Anti-inflammation treatment for protection of hepatocytes and amelioration of hepatic fibrosis in rats. Exp Ther Med 22: 1213, 2021.
13. Krishna M: Histological grading and staging of chronic hepatitis. Clin Liver Dis (Hoboken) 17: 222-226, 2021.
14. Radosavljevic T, Vukicevic D, Djuretić J, Gopcevic K, Labudovic Borovic M, Stankovic S, Samardzic J, Radosavljevic M, Vucevic D and Jakovljevic V: The role of macrophage inhibitory factor in TAA-induced liver fibrosis in mice: Modulatory effects of betaine. Biomedicines 12: 1337, 2024.
15. Wen SL, Feng S, Tang SH, Gao JH, Zhang LH, Tong H, Yan ZP and Fang DZ: Collapsed reticular network and its possible mechanism during the initiation and/or progression of hepatic fibrosis. Sci Rep 6: 35426, 2016.
16. Kim JY, Jun JH, Park SY, Yang SW, Bae SH and Kim GJ: Dynamic regulation of miRNA expression by functionally enhanced placental mesenchymal stem cells promoteshepatic regeneration in a rat model with bile duct ligation. Int J Mol Sci 20: 5299, 2019.
17. Yang YT, Ji MR, Lin ZJ, Li P, Wu RZ, Liu XD and Liu L: Bile duct ligation impairs visual acuity in rats by ammonia- and bilirubin-induced retinal degeneration. Acta Pharmacol Sin 46: 380-392, 2025.
18. Najibi A, Rezaei H, Manthari RK, Niknahad H, Jamshidzadeh A, Farshad O, Yan F, Ma Y, Xu D, Tang Z, *et al*: Cellular and mitochondrial taurine depletion in bile duct ligated rats: A justification for taurine supplementation in cholestasis/cirrhosis. Clin Exp Hepatol 8: 195-210, 2022.
19. Patel C, Shahgond L, Acharya S, Boddu SH and Ranch K: Protective effect of probiotics and ascorbic acid on bile duct ligation-induced chronic hepatic encephalopathy in rats. Res Pharm Sci 17: 445-456, 2022.

20. Wan X, Fang Y, Qin M, Zheng Q, Yang Q, Peng M, Hao M, Wang K, Zhao R, Shi Y, *et al*: Protective effect of MP-40 mitigates BDL-induced hepatic fibrosis by inhibiting the NLRP3-mediated pyroptosis. Front Pharmacol 15: 1479503, 2024.
21. Zhang N, Niu W, Niu W, Li Y, Guo S, Li Y, He W and He H: Isovalerylspiramycin I alleviates liver injury and liver fibrosis by targeting the nucleotide-binding protein 2 (NUBP2)-vascular non-inflammatory molecule-1 (VNN1) pathway. J Pharm Anal 15: 101048, 2025.
22. Pun CK, Huang HC, Chang CC, Hsu SJ, Chuang CL, Huang YH, Hou MC and Lee FY: Low-dose alcohol exacerbates hyperdynamic circulation and shunting in non-alcoholic cirrhotic rats. Biosci Rep 44: BSR20240354, 2024.
23. Semenovich DS, Zorova LD, Abramicheva PA, Andrianova NV, Elchaninov AV, Petrukhina AS, Pevzner IB, Manskikh VN, Zorov DB and Plotnikov EY: Impact of intermittent fasting and dietary restriction on redox state, energetic metabolism, and liver injury in common bile duct ligation model. Antioxidants (Basel) 13: 835, 2024.
24. Hajiasgharzadeh K, Shahabi P, Karimi-Sales E and Alipour MR: Nicotine promotes development of bile duct ligation-induced liver fibrosis by increasing expression of nicotinic acetylcholine receptors in rats. Clin Exp Hepatol 10: 62-71, 2024.
25. Roeb E: Matrix metalloproteinases and liver fibrosis (translational aspects). Matrix Biol 68-69: 463-473, 2018.
26. Suckow MA, Wilson RP, Hankenson FC and Foley PL: The laboratory rat. Elsevier, 2019.
27. Verhoven B, Zeng W, Chlebeck P, Matkowskyj K, Jennings H, Poore S and Al-Adra D: Heterotopic auxiliary whole liver rat transplant model utilizing a hepaticoureterostomy for allograft rejection studies. J Vis Exp: 10.3791/66516, 2024.
28. Zou Y, Yue P, Cao H, Wu L, Xu L, Liu Z, Wu S and Ye Q: A novel ameliorated rat model of reversible obstructive jaundice. J Zhejiang Univ Sci B 24: 345-351, 2023.
29. Du Y, Chen H, Xuan Z, Song W, Hong L, Guo D, Li H, Tuo B, Zheng S and Song P: Bile deficiency induces changes in intestinal glucose absorption in mice. Surgery 160: 1496-1507, 2016.
30. Lyu SC, Wang J, Xu WL, Wang HX, Pan F, Jiang T, He Q and Lang R: Therapeutic effect of combining anisodamine with neostigmine on local scar formation following Roux-en-Y choledochojejunostomy in a novel rat model. Front Pharmacol 12: 700050, 2021.
31. Huang X, Li CH, Zhang AQ, Kong Z, Gu WQ and Dong JH: A simple rat model of in situ reversible obstructive jaundice in situ reversible obstructive jaundice model. Ann Surg Treat Res 92: 389-395, 2017.
32. Luo WW, Zhou XL, Wang QQ, Shao YJ, Li ZM, Zhao DK and Yu SP: The application of Compont gel in chronic obstructive jaundice rats model. Acta Cir Bras 34: e201900504, 2019.
33. Apostu RC, Ciuce CC, Făgărăşan V, Scurtu RR and Ciuce C: Hepatoportoenterostomy in selective obstructive cholestasis-an new experimental model in the rat. Chirurgia (Bucur) 115: 252-260, 2020.